

## ● A point-by-point response to the reviews

**First of all, we would like to thank the reviewers for the helpful comments and suggestions. We are very appreciative of that. Our responses to the comments are in bold font. In the revised manuscript, the modifications are highlighted in red font.**

Anonymous Referee #1

Received and published: 8 June 2018

General comments

This paper presents results from a statistical study of ULF waves in the Pc5-Pc6 frequency range in the magnetotail using magnetic field and plasma data from instruments onboard the THEMIS satellite during 2008–2015. Azimuthally oscillating waves and radially oscillating waves are studied separately. The authors found that in the near-Earth magnetotail the dawn-dusk asymmetry of wave occurrence is observed only in the case of radially oscillating waves. In the far magnetotail, they reveal a higher occurrence rate during post-midnight magnetic local times than during pre-midnight, and that the peak frequency of waves decreases with increasing radial distance from Earth. A majority of events in the near-Earth magnetotail are standing waves, while these represent very small percentage of the events in the far magnetotail. No dawn-dusk asymmetry could be found in the wave frequencies. Finally, the authors studied the effects of solar wind parameters and geomagnetic activity, and found that ULF wave occurrence is favoured by high solar wind speed, high solar wind pressure variability, but quiet to moderately active geomagnetic activity.

Overall, the paper is well-written, the reasoning is clearly exposed, and it reaches substantial conclusions. Below are a few specific comments which could be considered to improve the manuscript before final publication.

Specific comments (major)

(I) It would be good to have a figure in the same format as Figure 3 showing the number of events in each bin, both for azimuthal and radial oscillating events. Indeed, the text mentions on several occasions that a given bin should be considered with caution due to the small number of events it contains. In particular, such an additional figure could help in analysing Figure 4, as one might want to be cautious in drawing conclusions with so many blank bins in this figure.

**We have added the distribution of event numbers in Fig. 3 in the revised manuscript. Two sentences**

**have been added in lines 173-175: “Figure 3a and 3b shows the spatial distribution of the number of events in the GSM\* X-Y plane, both for azimuthal (left panel) and radial (right panel) oscillating wave events. The blank bins inside the magnetopause indicate that there are no events.”.**

(II) l. 327: "solar wind dynamic pressure (Pd) and the IMF Bz values were also examined (not shown)." ! If the results on the dynamic pressure are mentioned in the conclusion (see l. 386), I would recommend to show the analysis of these parameters in the paper.

**Thanks for your suggestions. The relationship between the occurrence of ULF waves and the relative variation of solar wind dynamic pressure (Pd) and the IMF Bz values have been added in Fig. 8 (Fig. 8c and 8d) in the revised manuscript. And the calculation formula of the relative variation of Pd have been added in lines 347-349 in the revised manuscript.**

Specific comments (minor)

- l. 42: I suggest to give the frequency range for ULF waves from the very beginning of the introduction.

**The frequency range for ULF waves have been added in line 42 in the revised manuscript.**

- l. 69: The full name of THEMIS should be given when mentioned for the first time after the abstract (see AnGeo guidelines: [https://www.annales-geophysicae.net/for\\_authors/manuscript\\_preparation.html](https://www.annales-geophysicae.net/for_authors/manuscript_preparation.html)).

**Ok. The full name of THEMIS has been added in lines 69-70 in the revised manuscript.**

- l. 75: Please define MLT.

**The definition of MLT have been added in line 75 in the revised manuscript.**

- l. 77 and 79: "Susumu Kokubun (2013)" ! please check the reference. I think it should be "Kokubun (2013)", and in the reference list it should appear as "Kokubun, S. (2013). ULF waves in the outer magnetosphere...".

**Yes, revised.**

- l. 82: Pi2 should be defined.

**Ok. The definition of Pi2 have been added in line 83 in the revised manuscript.**

- l. 108: It could be worth briefly defining the GSM coordinate system here.

**Ok. The definition of GSM coordinate system has been added in lines 115-119 in the revised manuscript.**

- l. 120: I assume Dp stands for "dynamic pressure"; perhaps it would be better to make it fully clear to the reader.

**Yes, it stands for "dynamic pressure". The full name of Dp has been added in line 112 in the revised manuscript.**

- Figure 2: I would suggest that, for a given event (A/B), the three components of the velocity, magnetic field, electric field should have the same y-axis limits. This would better emphasise the azimuthal or radial nature of the oscillations. This could also be done for the components of the PSD of the velocity, as the relative importance of the peaks would be immediately visible, without needing to look at the scale for comparison. An exception should obviously be made for panel (d2), as the Bz range for event B is very large.

**Ok. We re-plotted Fig. 2 using the same y-axis limits for the components of each vector quantity (except Bz) in the revised manuscript.**

- l. 174: "calculated by dividing the total event times by the total observation times" ! do you mean the total number of events/observations? Or the total duration of events/observations? This wording may be ambiguous; please rephrase.

**Ok. The sentence has been rephrased as "calculated by dividing the total duration of all events by the total duration of observations in each bin" in line 183 in the revised manuscript.**

- l. 177: "For azimuthal oscillating events, there is no clear dawn-dusk asymmetry in the occurrence rates" ! based on Figure 3, this statement seems a bit too strong, since high occurrence rates (red colour) span within 18–20 MLT on the duskside vs 5–6 MLT on the dawnside. Perhaps rephrasing this statement into something like "For azimuthal oscillating events, the dawn-dusk asymmetry in the occurrence rates is less clear than for radial oscillating events" would be better. Similarly, this statement should also be made less strong in the conclusion and abstract.

**Thank you, the sentence has been rephrased as "For radial oscillating events, the occurrence rates of waves are higher on the duskside than dawnside. For azimuthal oscillating events, the dawn-dusk asymmetry in the occurrence rates is less clear than that for radial oscillating events." in lines 187-189 in the revised manuscript. Similarly, the sentence has also been rephrased in lines 281-283 and 397-399 in the revised manuscript.**

- l. 202: "the frequency can be as low as 0.55 mHz" which is the lower frequency in the Pc6 band retained in this study. Could there be waves with even lower frequency observed? To my knowledge, there is no upper limit in the period of Pc6 oscillation (see Saito, T. (1978), Long-period irregular magnetic pulsation, Pi3, Space Sci. Rev., 21(4), 427–467, doi:10.1007/BF00173068), so it could be interesting to check whether pulsations of even lower frequency can be identified.

The field aligned coordinates used in this work are obtained by subtracting the 30min sliding average background magnetic field. So, we only focus on waves with frequencies above 0.55mHz. However, in the preliminary screening stage, we did notice two wave events with frequencies as low as 0.49 mHz and 0.51mHz, which can be studied in the future work. Besides, the words “Pc6 (>600s)” were revised in line 57 in the revised manuscript. The paper of Saito (1978) was quoted in the lines 58 and 496-497 in the revised manuscript.

- l. 226: "The second row shows the 1.26-3.26 mHz (Fig. 6a) and 2.03-4.03 mHz (Fig. 6b) band-pass filtered Ba and Er components"!how were those frequency bands selected?

The lower (upper) limit of the frequency bands is obtained by subtracting (adding) 1 mHz from the peak frequency in Fig. 2(l-n). We added one sentence in lines 237-238.

- l. 319-320: The calculation of the normalised event number does not seem fully clear to me. Is it so that the number of events is divided by the proportion of solar wind speed within a given bin to the total duration of solar wind measurements? Or are events binned according to the mean/median solar wind speed at the time when they were observed? Please rephrase this explanation.

Yes, the detailed calculation formula for the normalized event number is as follows (take that dividing by the duration proportion of solar wind Vx as an example):

$$\begin{aligned} \text{Normalized event number} &= \frac{\text{the number of events in a given bin}}{\text{the duration proportion of solar wind Vx in a given bin}} \\ &= \frac{\text{the number of events in a given bin}}{\frac{\text{duration of background Vx in a given bin}}{\text{total duration of background Vx}}} \end{aligned}$$

Taking into account the suggestion of another reviewer, we re-plotted Figure 8. The new vertical axis shows the probability of detecting a wave event instead of the normalized number of events in each bin. The probability is calculated by dividing the normalized event number in a given bin by the total normalized event number of all bins (take the solar wind Vx as an example). The sentence has been rephrased to “The Y-axis indicates the probability of detecting one wave event in each bin. The background solar wind data is obtained from OMNI from 2008 to 2015.” in lines 338-339 in the revised manuscript.

Copyediting and typesetting

All the following problems have been corrected in the revised manuscript accordingly.

- l. 57: "primarily" being an adverb, it cannot be used in this context. Instead, one could write, for instance, "Pc5 and Pc6 waves are the most common waves observed at high latitudes and in the

magnetotail."

- l. 60: "nightside" is generally written in a single word (same for dawnside, dayside, duskside...)
- l. 67: "the both occurrence and frequency distributions..." → "both the occurrence and frequency distributions..."
- l. 102, l. 201: earth ! Earth
- l. 106: sub-solar ! subsolar
- l. 108: "whose X axis **is** rotated"
- l. 145: "to satisfy **the** criteria mentioned above"
- l. 154: "of **the** three components"
- l. 260: "the magnetic field lines in the nightside **are** very stretched"
- l. 276: "K-H instabilities are **more** inclined to occur in the dawnside than in the duskside"
- l. 278: "more events are needed **to** further study the definite reasons"
- l. 286: Alfvén ! Alfvén
- l. 321: "the ULF waves occurrences increase with" ! "the ULF wave occurrence increases with"
- l. 322: a sources ! a source
- l. 324: "the waves occurrences are higher" ! "the wave occurrence is higher"
- l. 327: occurrence
- l. 336: (Forsyth et al., 2015) ! Forsyth et al. (2015)
- l. 379: "the peak frequency decreases **with increasing** radial distance"
- l. 383: "the frequencies for all the events in this paper do not show obvious dawndusk asymmetry **contrary to results from** previous studies for waves in the inner magnetosphere" (the original phrasing can be ambiguous and interpreted the other way round)
- l. 387: maybe ! may be
- l. 389: "that the ULF waves **are** most likely to occur"

Anonymous Referee #2

Received and published: 11 June 2018

This paper presents a statistical analysis of ULF waves in the nightside magnetosphere including the tail region up to geocentric distances of 32 Re. The wave events are identified using plasma bulk velocity data to capture fundamental field line oscillations. The wave events are classified into radial and azimuthal type and standing and nonstanding modes. The most important result is the finding that standing waves are hardly detected beyond 16 Re. I find this result to be very interesting and significant. I recommend publication of the manuscript after the authors have considered minor comments listed below.

Line 78. Please change “Susumu Kokubun” to “Kokubun”

**Revised.**

Line 136. “quasi monochromatic” Is this judgement made by visual inspection of the time series data? If so, it may explain some discrepancies between the present and previous studies (see my comment on line 267 below).

**Thanks for your suggestions. In this study, the “Quasi monochromatic” is not exactly made by visual inspection of the time series data. We conduct Fast Fourier Translation (FFT) analysis to all the candidate time series as to the event shown in Fig. 2(l-n). Then, we judge whether there is an obvious spectral peak in FFT spectrum by visual inspection. Only events with an obvious single spectral peak are considered as “quasi monochromatic” wave. We added one sentence in lines 158-159.**

Line 169, Figure 2. I recommend using a common amplitude scale for the components of each vector quantity. It makes easier to visually grasp the amplitude difference between the toroidal and poloidal components.

**Ok. Figure 2 has been re-plotted by using the same y-axis limit for each component in the revised manuscript.**

Line 171. The  $E_z$  component is not zero. This should be pointed out in the main text and explained in relation to how you define the field line coordinate system.

**Thanks for your suggestion. The sentence has been added in lines 163-166 in the revised manuscript: “Note that the magnetic field vector used for calculating  $E$  ( $E = -\delta V \times B$ ) at each moment may be**

deviate from the z-axis determined by 30 minutes sliding average of the magnetic field data. Therefore, the  $E_z$  component will have a little deviation from zero in the FAC coordinate system as shown in Fig. 2g.”

Line 232. The phase difference can be  $\sim -90$  degrees, depending on the magnetic latitude (or distance from the tail midplane where  $B_x = 0$ ). I hope that events exhibiting this phase delay are also included.

**Thanks for your comments. The events with  $-90^\circ$  phase difference have already been included in our list of events. Because either the phase deference of  $\sim 90^\circ$  or  $-90^\circ$  is considered as the characteristic of a standing wave. We rephrased the words “the phase differences” as “the absolute value of the phase differences” in lines 238 and 243 in the revised manuscript.**

Line 239. I guess that this probability means the probability that a given azimuthal or radial wave event shows signatures of a standing wave, not the probability that you find a standing wave at a given time. Please clarify.

**Yes, the sentence has been rephrased as “Figure 7 shows the radial distribution of the probability that a given azimuthal or radial oscillating wave event shows signatures of a standing wave.” in lines 249-250 in the revised manuscript.**

Line 240. Change “deep” to something like “dark”

**Revised. See line 250 in the revised manuscript.**

Line 259. “fundamental eigenmode”. You can justify this mode identification by examining the relationship between the sign of the  $E_r$ - $B_a$  phase difference and the magnetic latitude of the spacecraft. You can also identify second harmonic from the phase difference. Have you found any second harmonic waves? Second harmonic poloidal (radial) waves have been reported at  $R < 10$  (e.g., Hughes et al., 1979), and I wonder if you have encountered any at  $R > 10$ .

Hughes, W. J., McPherron, R. I., Barfield, J. N., & Mauk, B. H. (1979). A compressional Pc4 pulsation observed by three satellites in geostationary orbit near local midnight. *Planetary and Space Science*, 27(6), 821-840. doi:10.1016/0032-0633(79)90010-2

**Thanks for your suggestions. According to your suggestion, we try to identify the second harmonic waves by the E-B phase difference and the magnetic latitude. Figure S1 is a schematic diagram describing the latitude dependence of phase difference for the fundamental waves and second harmonic waves. We can see that the sign of E-B phase difference between the fundamental waves and second harmonic waves is opposite at the same observation latitudes. The azimuthal oscillating wave could be second harmonic wave if  $E_r$  lead (lag)  $B_a$  by  $\sim 90^\circ$  when  $MLAT < 0$  ( $MLAT > 0$ ), and the radial oscillating wave could be second harmonic if  $E_a$  lead (lag)  $B_r$  by  $\sim 90^\circ$  when  $MLAT > 0$  ( $MLAT < 0$ ). In total, we find that about 3.03% (33) azimuthal oscillating wave events may be second**

harmonic waves and 2.65% (15) radial oscillating wave events may be second harmonic waves, as shown in Figure S2. The above analysis result is not contradictory to our opinion that most of our standing wave events are fundamental waves. We added two sentences about the harmonic mode in lines 270-272 in the revised manuscript.

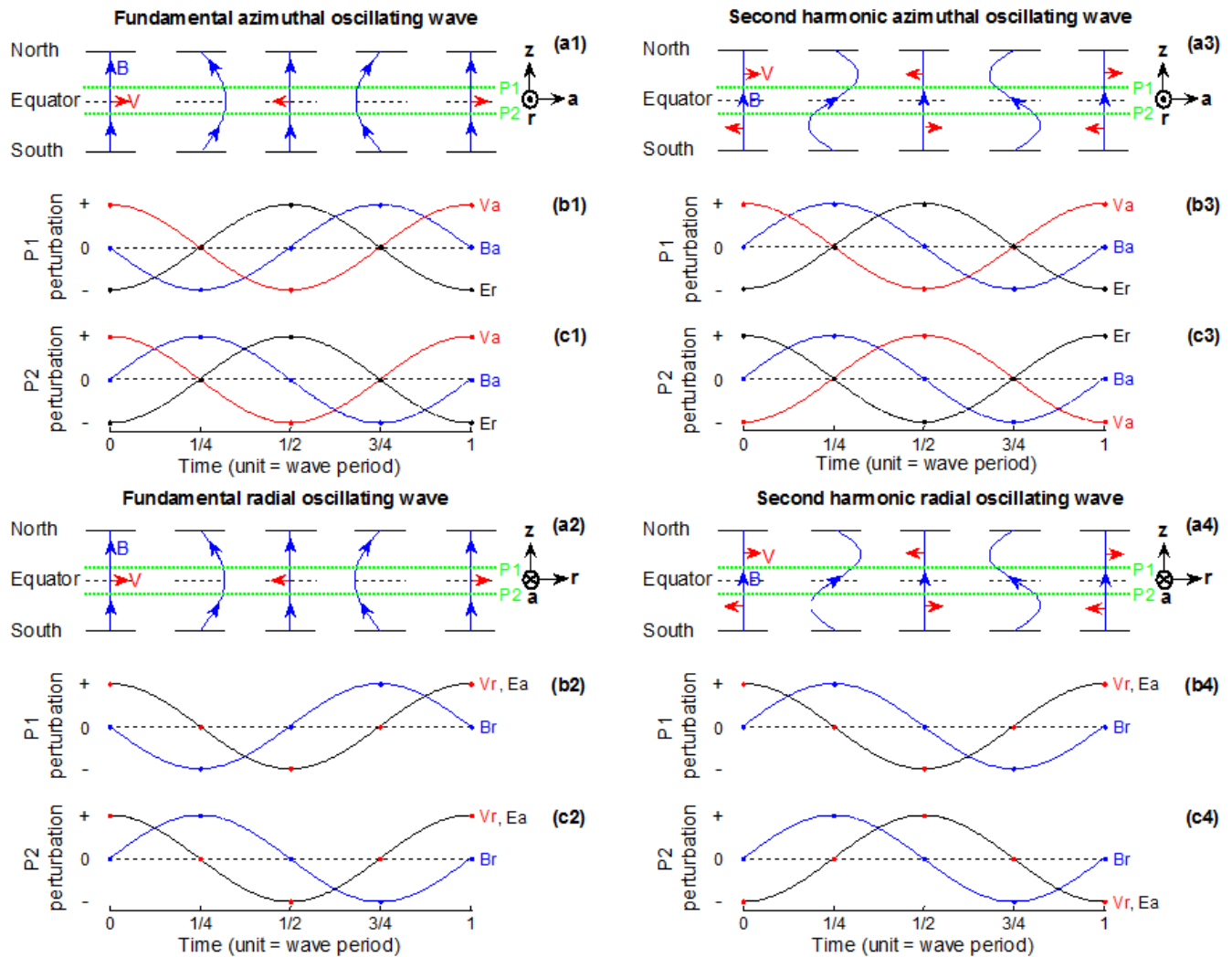


**Figure S1.** (a1) Schematic illustration of magnetic field B (blue line) and velocity V (red arrow) for the fundamental azimuthal oscillating wave in the magnetic meridian plane. The black dashed line indicates the magnetic equator plane, and the green dashed line P1 (P2) indicates a fixed point slightly on the north (south) side of the magnetic equator plane. (b1) The temporal variation of Ba, Va and Er at the P1 point. (c1) The temporal variation of Br, Vr and Ea at the P2 point. (a2-c2) are the same as (a1-c1), but for the fundamental radial oscillating wave. (a3-c3) and (a4-c4) are the



same as (a1-c1) and (a2-c2), but for the second harmonic oscillating waves. Refer to Fig. 3 of Takahashi et al. (2014).

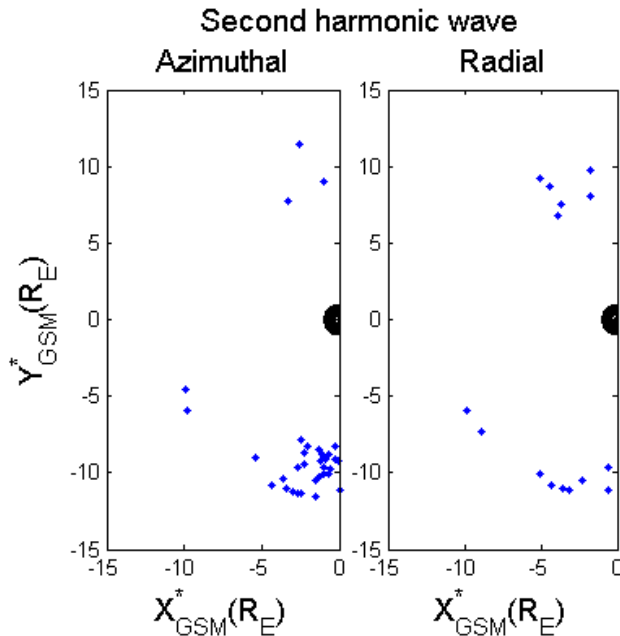


**Figure S2. The distribution of second harmonic waves in the GSM\* X-Y plane.**

Line 267. This is different from the Geotail result obtained by Kokubun (2013, Figure 15) and Takahashi et al. (2014, doi:10.1002/2014ja020274, Figure 5). Please comment on this difference and offer explanation if possible.

**Kokubun (2013, Figure 15) shows that the number of waves is higher on the dawnside than duskside, at first glance, it is different from our results. We noticed that, in his work, the orbit normalization was not conducted and the events they focused on mainly occur in the dayside. The number of events (153) observed in the nightside is less in his work, which is probably because the amplitude of waves is required to be greater than 30 km/s in his work, while the amplitude of waves should be greater than 25 km/s in our study.**

**Takahashi et al. (2014, Figure 5) shows that the occurrence rate of toroidal waves is higher on the dawnside than duskside and the occurrence rate is zero in the midnight region, which are different from our results. The possible reason is that they only focused on the pure toroidal wave, while azimuthal oscillating waves with comparable power in  $V_a$  and  $V_r$  are also included in our list of events. Thus, more azimuthal oscillating waves could be observed in the duskside in our study, because of the possible coupling between azimuthal oscillating waves and radial oscillating waves**

(with higher occurrence in the dusk sector). Another possible reason for these differences is that their waves were identified automatically by program using a 60 min data window and there was no precise beginning and ending time. A quantitative standard is used in our study to determine the beginning and ending time of each event, which may lead to a different list of events between our than their works. We added some additional comments in lines 287-292 in the revised manuscript.

Line 287. “Poulters” means “Allan and Poulter?”

Yes, revised.

Line 298, “Highly stretched field lines”. Is it possible that some events are observed on open field lines?

It is an interesting question. However, we can only say statistically that the events we studied were happened on closed magnetic field lines. We have calculated the elevation angle of the magnetic field line for all wave events as shown in Fig. S3. It found that 61.70% of the events have an elevation angle larger than  $45^\circ$  and only 2.48% events with an elevation angle  $<10^\circ$ . It suggests that most of our events are observed near the magnetic equatorial plane. In addition, we mainly use ion velocity data to identify ULF waves, which are usually reliably measured in the plasma sheet. Therefore, it is unlikely that the events studied in this work were occurred on open magnetic field lines. We added some additional comments in lines 269 and 273-277 in the revised manuscript.

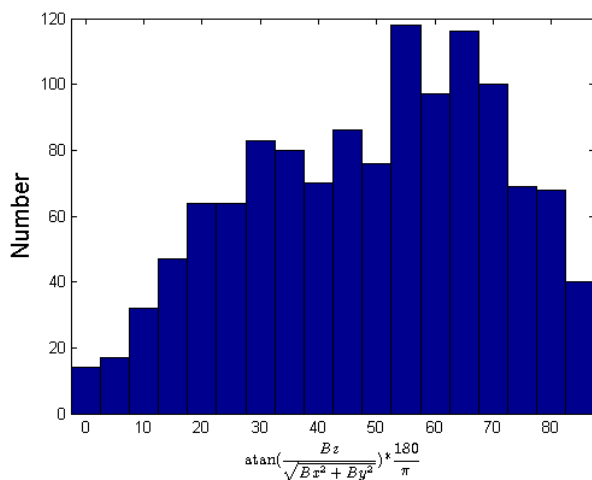


Figure S3. The distribution of elevation angle of the magnetic field line.

Line 331. Figure 8. It would be better if the vertical axis shows the probability of detecting a wave event (instead of the number of events) in each bin for the solar wind velocity and AE index.

Thanks for your suggestion. we have re-plotted Fig. 8. The new vertical axis shows the probability of detecting a wave event instead of the normalized number of events in each bin. The detailed calculation formula for the probability is as follows (take the solar wind Vx as an example):

$$\begin{aligned} \text{Normalized event number} &= \frac{\text{the number of events in a given bin}}{\text{the duration proportion of solar wind Vx in a given bin}} \\ &= \frac{\text{the number of events in a given bin}}{\frac{\text{duration of background Vx in a given bin}}{\text{total duration of background Vx}}} \end{aligned}$$

$$\text{Probability} = \frac{\text{the normalized event number in a given bin}}{\text{the total normalized event number of all bins}}$$

The sentence has been rephrased to “The Y-axis indicates the probability of detecting one wave event in each bin. The background solar wind data is obtained from OMNI from 2008 to 2015.” in lines 338-339 in the revised manuscript.

## ● A list of all relevant changes made in the manuscript

Line 42. The frequency range for ULF waves was added.

Line 57. “Pc6 (600-1800s)” ! “Pc6 (>600s)”. “primarily” ! “most common”

Line 58. The paper of Saito (1978) was quoted.

Line 60. “dusk side” ! “duskside”, “dawn side” ! “dawnside”, “night side” ! “nightside” in the full text.

Line 67. “the both” ! “both the”.

Line 69. The full name of THEMIS was added.

Line 75. The definition of MLT was added.

Line 77. “Susumu Kokubun, 2013” ! “Kokubun, 2013”.

Line 79. “Susumu Kokubun (2013)” ! “Kokubun (2013)”

Line 82. The definition of Pi2 was added.

Line 103. “earth” ! “Earth”.

Line 107. “sub-solar” ! “subsolar”.

Line 112. The full name of Dp was added. “npa”! “nPa”.

Line 115. "whose X axis is rotated".

Lines 115-119. The definition of GSM coordinate system was added

Line 148. "to satisfy the criteria mentioned above".

Line 157. "of the three components".

Line 158. The explanation of “quasi monochromatic” was added.

Line 163. The explanation of “The Ez component is not zero” was added.

Line 167. We re-plotted Fig. 2 using the same y-axis limits.

Line 173. We added the description of Fig. 3a and 3b.

Line 183. “event times” ! “duration of all events”, “observation times” ! “duration of observations in each bin”

Line 184. We added the description of blank bins in Fig. 3c and 3d.

Line 187. We rephrased the statement about the distribution of occurrence rates of azimuthal oscillating waves in the near-earth region. This statement was also rephrased in lines 281 and 397.

Line 194. We re-plotted Fig. 3 and added the distribution of event numbers.

Line 211. “earth” ! “Earth”

Line 237. The method of selecting the frequency bands was added.

Lines 238 & 243. “the phase differences” ! “the absolute value of the phase differences”

Line 249. We rephrased the description of the Y-axis of Fig. 7.

Line 250. “deep” ! “dark”.

Lines 269-277. A few lines about “the harmonic mode” and “open magnetic field lines” were added.

**Line 287. We added the differences between our result and that of Takahashi et al. (2014), and discussed the potential reasons.**

**Line 275. "the magnetic field lines in the nightside are very stretched".**

**Line 296. "are more inclined to occur".**

**Line 299. "needed to further study".**

**Line 306. "Alfven" ! "Alfvén", "Poulters" ! "Allan and Poulter"**

**Line 338. We rephrased the description of Y-axis of Figure 8.**

**Line 340. "the ULF waves occurrences increase with" ! "the ULF wave occurrence increases with"**

**Line 341. "a sources" ! "a source".**

**Line 342. "the waves occurrences are higher" ! "the wave occurrence is higher".**

**Line 346. "occurrences" ! "occurrence".**

**Line 347. The calculation formula of the relative variation of Pd was added.**

**Line 351. We re-plotted Fig. 8. The relationship between the occurrence of ULF waves and the relative variation of Pd and the IMF Bz values were added. The new Y-axis shows the probability of detecting a wave event instead of the normalized number of events.**

**Line 357. "(Forsyth et al., 2015)" ! "Forsyth et al. (2015)".**

**Line 401. "decreases as the increase of radial distance" ! "decreases with increasing radial distance".**

**Line 406. "as found in previous studies" ! "contrary to results from previous studies".**

**Line 410. "maybe" ! "may be".**

**Line 412. "the ULF waves are most likely to occur"**

**Line 496. The paper of Saito (1978) was quoted.**

**Line 526. " Susumu, K" ! "Kokubun, S"**

**Line 532. The paper of Takahashi (2014) was quoted.**

## ● A marked-up manuscript version

# 1 Statistical study of ULF waves in the magnetotail by THEMIS 2 observations

3  
4 Shuai Zhang<sup>1,2</sup>, Anmin Tian<sup>1\*</sup>, Quanqi Shi<sup>1</sup>, Hanlin Li<sup>1</sup>, Alexander W. Degeling<sup>1</sup>, I. Jonathan Rae<sup>3</sup>, Colin  
5 Forsyth<sup>3</sup>, Mengmeng Wang<sup>1</sup>, Xiaochen Shen<sup>1</sup>, Weijie Sun<sup>4</sup>, Shichen Bai<sup>1</sup>, Ruilong Guo<sup>5</sup>, Huizi Wang<sup>1</sup>,  
6 Andrew Fazakerly<sup>3</sup>, Suiyan Fu<sup>6</sup>, Zuyin Pu<sup>6</sup>

7  
8 <sup>1</sup>Shandong Provincial Key Laboratory of Optical Astronomy and Solar-Terrestrial Environment, School of Space  
9 Science and Physics, Shandong University, Weihai, 264209, China

10 <sup>2</sup>State Key Laboratory of Space Weather, Chinese Academy of Sciences, Beijing 100190, China

11 <sup>3</sup>University College London, Mullard Space Science Laboratory, Space and Climate Physics, Dorking, United  
12 Kingdom

13 <sup>4</sup>Department of Climate and Space Sciences and Engineering, University of Michigan, Ann Arbor, USA

14 <sup>5</sup>Institute of Geology and Geophysics Chinese Academy of Sciences, Beijing 100029, China

15 <sup>6</sup>School of Earth and Space Sciences, Peking University, Beijing 100871, China

16  
17 \* *Correspondence to:* A. M. Tian (tamin@sdu.edu.cn)

18  
19 **Abstract.** Ultra-low frequency (ULF) waves are ubiquitous in the magnetosphere. Previous studies  
20 mostly focused on ULF waves in the dayside or near-earth region (with radial distance  $R < 12 R_E$ ). In this  
21 study, using the data of Time History of Events and Macroscale Interactions during Substorms (THEMIS)  
22 during the period from 2008 to 2015, the Pc5-6 ULF waves in the tail region with  $X^*_{GSM} < 0$ ,  $8 R_E < R <$   
23  $32 R_E$  (mostly on the stretched magnetic field lines) are studied statistically. A total of 1089 azimuthal  
24 oscillating events and 566 radial oscillating events were found. The statistical results show that both the  
25 azimuthal and radial oscillating events in the magnetotail region ( $12 R_E < R < 32 R_E$ ) are more frequently  
26 observed in the post-midnight region. The frequency decreases with increasing radial distance from Earth  
27 for both azimuthal oscillating events ( $8 R_E < R < 16 R_E$ ) and radial oscillating events ( $8 R_E < R < 14 R_E$ ),  
28 which is consistent with the field line resonances theory. About 52 % of events (including the azimuthal  
29 and radial oscillating events) are standing waves in the region of 8-16  $R_E$ , while only 2 % are standing  
30 waves in the region of 16-32  $R_E$ . There is no obvious dawn-dusk asymmetry of ULF wave frequency for  
31 events in  $8 R_E < R < 32 R_E$ , which contrasts with the obvious dawn-dusk asymmetry found by previous  
32 studies in the inner magnetosphere ( $4 R_E < R < 9 R_E$ ). An examination for possible statistical relationships  
33 between ULF wave parameters and substorm occurrences is carried out. We find that the wave frequency  
34 is higher after the substorm onset than before it, and the frequency differences are more obvious in the  
35 midnight region than in the flank region.

36

37 **Keyword.** Magnetospheric physics (Magnetotail; MHD waves and instabilities; Solar wind-  
38 magnetosphere interactions)

39

## 40 **1 Introduction**

41

42 Ultra-low frequency (ULF) waves **with frequencies between about 1mHz and 5 Hz** play a significant role  
43 in storing and transferring energy in the Earth's magnetosphere. ULF waves can transport energy from  
44 the magnetosphere to the ionosphere, accelerate energetic particles, modulate luminosity of aurorae,  
45 mediate reconnection and trigger substorm onset (e.g., Baumjohann and Glassmeier, 1984; Lessard et al,  
46 1999; Ukhorskiy et al., 2005; Keiling, 2009; Rae et al., 2014; Zong et al., 2009; Zong et al., 2017).

47 There are several excitation sources for magnetospheric ULF waves. These sources include the  
48 Kelvin-Helmholtz instability (KHI) along the magnetopause (e.g., Walker, 1981; Claudepierre et al.,  
49 2008), solar wind dynamic pressure impulse (e.g., Allan et al., 1986; Lee et al., 1989; Zhang et al., 2010;  
50 Zong et al., 2012; Shi et al., 2013, 2014; Degeling et al., 2014; Shen et al., 2015), periodic solar wind  
51 dynamic pressure variations (e.g., Kepko,2002; 2003), drift-bounce resonance (e.g., Southwood et  
52 al.,1969; Yang et al., 2010) and dynamic processes during substorms (e.g., Olson, 1999; Sun et al., 2015).

53 Although many previous studies have focused on waves occurring in the dayside magnetosphere  
54 (e.g., Samson et al., 1981; Rostoker et al., 1984; Zong et al., 2007; Shen et al., 2017), ULF waves  
55 occurring on stretched magnetic field lines in the magnetotail have also been reported in some  
56 observational studies (e.g., Zheng et al., 2006; Tian et al., 2012) and simulations (e.g., Rankin et al., 2000;  
57 Lui and Cheng, 2001). Pc5 (150-600 s) and Pc6 (**>600s**) waves are the **most common** waves occurring at  
58 high latitudes and in the magnetotail (**Saito, 1978**). Investigating the source and characteristics of these  
59 waves in the magnetotail will help us further understand the solar wind-magnetosphere-ionosphere  
60 coupling processes in the **nightside** region.

61 Statistical studies of ULF wave properties in the magnetosphere have been performed using various  
62 satellites (e.g., Hudson et al., 2004; Liu et al., 2009; Takahashi et al., 2015). Hudson et al. (2004)  
63 performed a statistical study of the occurrence rate of Pc5 magnetic pulsations for both toroidal and  
64 poloidal modes at L values from 4 to 9 by using 14 months magnetometer data from Combined Release  
65 and Radiation Effects Satellite (CRRES). They found that there is no dawn-dusk asymmetry on the  
66 occurrence rate of toroidal mode oscillations inside L=8, however the occurrence rate of poloidal mode  
67 oscillations is higher on **dusk**side. Liu et al. (2009) statistically studied **both the** occurrence and frequency  
68 distributions of Pc5 magnetic pulsations in toroidal and poloidal modes between L= 4 and 9 by using 13  
69 months electric and magnetic field measurements from **Time History of Events and Macroscale**  
70 **Interactions during Substorms (THEMIS)**. They found that the occurrence distribution is similar to the  
71 results of Hudson et al. (2004) and the frequency is higher in the **dawn**side than in the **dusk**side by a factor  
72 2 and decreases with radial distance. Takahashi et al. (2015) statistically investigated the fundamental

73 toroidal mode oscillations from  $L = 7$  to 12 by using 2008-2013 ion bulk velocity data from THEMIS-D.  
74 They found that the occurrence rate and amplitude of toroidal mode oscillations are higher in the **dawnside**  
75 (4-8 **magnetic local time (MLT, in hours)**) than in the **duskside** (16-20 MLT). Moreover, the relationship  
76 between ULF wave characteristics and the solar wind conditions/geomagnetic activity level were also  
77 studied statistically (e.g. Takahashi and Ukhorskiy. 2007; **Kokubun, 2013**; Wang et al., 2015). Takahashi  
78 and Ukhorskiy (2007) found that the solar wind dynamic pressure variance has the best correlation with  
79 the power of magnetic pulsations at geosynchronous orbit. **Kokubun (2013)** statistically studied Pc5 ULF  
80 waves (mostly on the 4-8 MLT and 16-20 MLT) using GEOTAIL data during the period of 1995 to 2000.  
81 They found that the wave occurrence tends to be larger for higher solar wind velocity ( $> 400$  km/s),  
82 smaller IMF  $B_z$ , and lower cone angle. Wang et al. (2015) studied the spatial distribution of the **irregular**  
83 **oscillations** Pi2 (40–150 s) and Pc4-5 magnetic fluctuation power in the plasma sheet by using THEMIS-  
84 A/C/D/E data from 2007 to 2014. They found that the amplitude of Pc-5 fluctuations is larger globally  
85 during periods of higher AE index, faster solar wind, and larger solar wind dynamic pressure variations.

86 Although statistical studies of ULF waves have been performed, most have focused on the dayside  
87 or near-earth region. The distributions and excitation mechanisms of ULF waves on stretched magnetic  
88 field lines are still unclear. Our work focuses on ULF waves on stretched magnetic field lines ( $X_{GSM}^* < 0$   
89 and  $8 R_E < R < 32 R_E$ ).

90 This paper will be organized as follows. In section 2, the data set and the selection criteria of the ULF  
91 wave event are presented. In section 3, we show the statistical results. In section 4, we discuss the  
92 occurrence and frequency distributions of ULF waves on the stretched field lines and the influence factors  
93 of solar wind parameters and geomagnetic activity level. The main conclusions of this study are given in  
94 section 5.

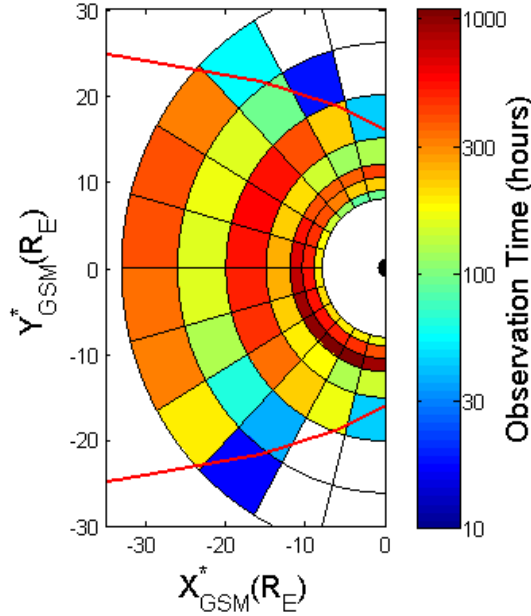
95

## 96 **2 Data and statistical methods**

97

98 In this study, we use 3 s resolution magnetic field data from Flux Gate Magnetometer (FGM) (Auster et  
99 al., 2008) and 3 s resolution plasma data from Electrostatic Analyzer (ESA) (Mcfadden et al., 2008) of  
100 THEMIS mission from 2008 to 2015. The THEMIS mission consists of five satellites (THEMIS  
101 A/B/C/D/E), each with an orbital inclination of about  $10^\circ$  (Angelopoulos, 2008). In the first two years,  
102 the apogees were about  $12 R_E$  for THEMIS A/D/E,  $20 R_E$  for THEMIS C and  $30 R_E$  for THEMIS B. After  
103 2010, THEMIS B/C were transferred to a lunar orbit which is about  $60 R_E$  from Earth. Because THEMIS  
104 A/D/E have similar orbits, in this study we only use data from THEMIS A, B and C. In addition, we use  
105 1 minute resolution interplanetary magnetic field (IMF) and solar wind plasma data from the OMNI  
106 database (<https://spdf.sci.gsfc.nasa.gov/>), which is calculated by time shifting satellite data taken in the  
107 solar wind to the Earth's bow shock **subsolar** point. Figure 1 shows the binned spatial distribution of the  
108 total observation time over the 2008-2015 interval for THEMIS A/B/C in the magnetosphere.





109  
 110 **Figure 1.** The distribution of total observation time of THEMIS A/B/C in the GSM\* X-Y plane between  
 111 2008 and 2015. The red line is the average magnetopause, calculated by Shue et al.'s (1998) model with  
 112 **dynamic pressure (Dp)** =1.66 nPa and Bz=0.16 nT. The blank bins indicate regions where the residence  
 113 time of THEMIS is less than 10 hours.

114  
 115 We use the aberration coordinate GSM\* whose X axis is rotated 4° from the X axis of **Geocentric**  
 116 **Solar Magnetospheric (GSM)** coordinates for spacecraft position to remove the effect of Earth's  
 117 revolution. In GSM coordinates, the X-axis is pointing from the Earth towards the Sun, the X-Z plane  
 118 contains the dipole axis, the Y-axis is perpendicular to the Earth's magnetic dipole, towards the dusk and  
 119 is included in the magnetic equatorial plane. Field-aligned coordinates (FAC) are used to analyze waves  
 120 and separate the azimuthal and radial oscillating wave components. The FAC system is defined in Eq. (1).

$$121 \quad \mathbf{z} = \frac{\mathbf{B}_0}{|\mathbf{B}_0|}; \mathbf{a} = \frac{\mathbf{z} \times \mathbf{R}}{|\mathbf{z} \times \mathbf{R}|}; \mathbf{r} = \mathbf{a} \times \mathbf{z} \quad (1)$$

122 In this equation,  $\mathbf{B}_0$  is the background magnetic field vector, derived by taking a 30 minutes sliding  
 123 average of the magnetic field data,  $\mathbf{R}$  is the vector from Earth's center to the satellite,  $\mathbf{z}$  is the parallel unit  
 124 vector,  $\mathbf{a}$  is the unit vector pointing east and  $\mathbf{r}$  completes the right-hand rule. It should be noted that the  
 125 direction of  $\mathbf{r}$  is approximately radial due to the equatorial orbits of THEMIS.

126 In this study, we mainly use ion velocity data to identify ULF waves, following the technique of  
 127 Takahashi (2015). They suggested that using velocity is better than using magnetic field data, because  
 128 fundamental mode magnetic field fluctuations (considered most likely in the Pc5 range) give rise to a  
 129 node near the equatorial plane, making their measurement problematic along the low-inclination THEMIS

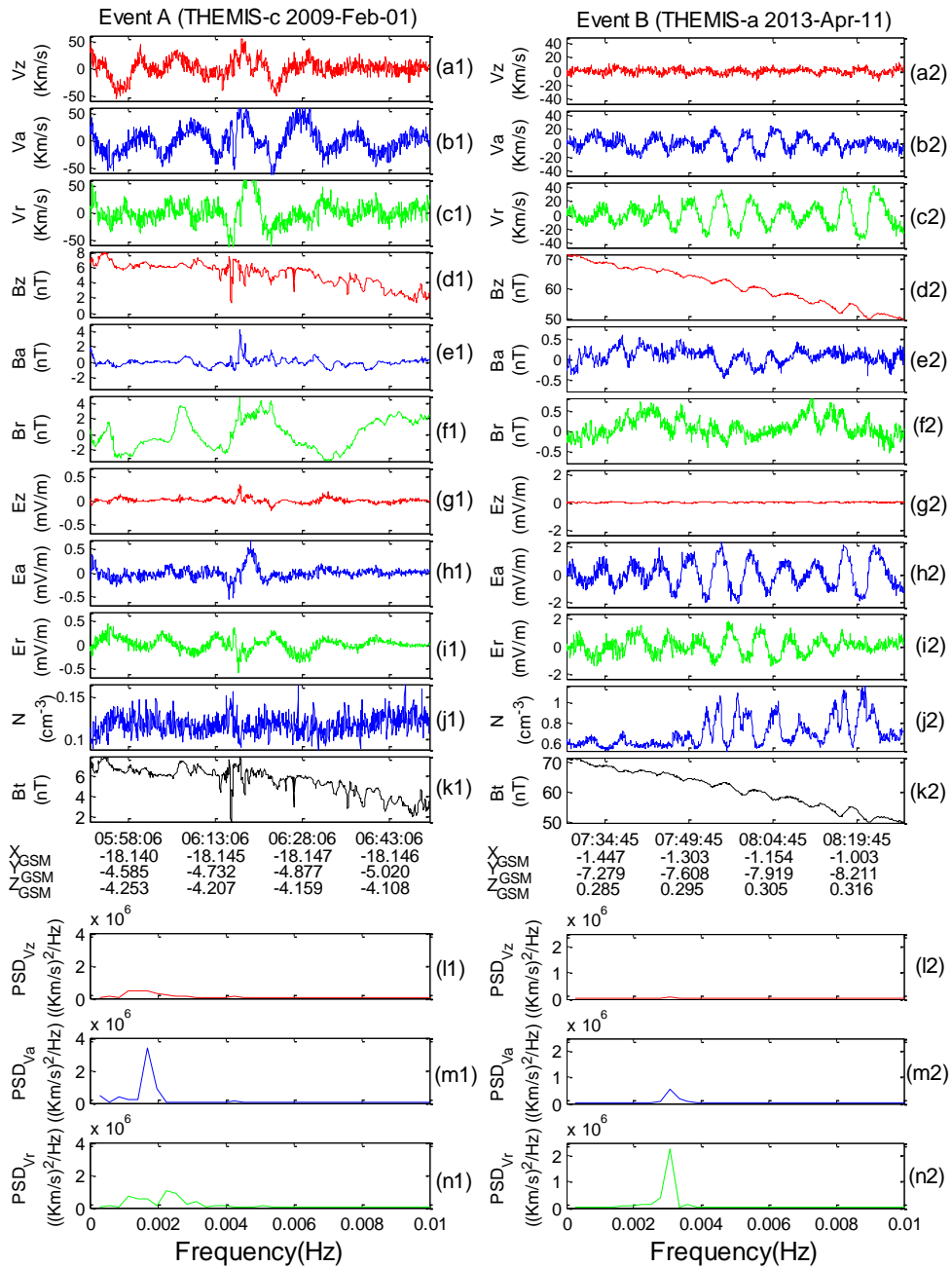
130 orbital path. On the other hand, the fundamental mode has an antinode for the electric field and plasma  
131 velocity fluctuations under ideal MHD conditions. The electric field data is therefore estimated by  $\mathbf{E} =$   
132  $-\delta\mathbf{V}\times\mathbf{B}$ , where  $\delta\mathbf{V}$  indicates the variation of velocity, which is obtained by subtracting the 30 minutes  
133 sliding average values.

134 As shown in Fig. 1, the region concerned in this work is  $X^*_{\text{GSM}} < 0 R_E$  and  $8 R_E < R < 32 R_E$ . In order  
135 to remove the likelihood of identification of ULF wave events when THEMIS enters the magnetosheath  
136 or solar wind regions, only events for which density values less than  $1 \text{ cm}^{-3}$  if  $|Y^*_{\text{GSM}}| > 10 R_E$  are included  
137 in the database.

138 The following criteria are used to select ULF waves in the magnetotail: (i) the wave frequency is  
139 below 7 mHz; (ii) the wave is quasi monochromatic, and includes at least three cycles; (iii) the maximum  
140 of peak to trough value of fluctuations is more than 50 km/s; (iv) mirror-like structures, indicated by anti-  
141 phase variations of magnetic field and density are excluded; (v) magnetotail flapping events, characterized  
142 by sign changes in  $B_x$  are excluded. A quantitative standard is used to determine the beginning and ending  
143 time of each event, namely that the beginning and ending time is at the points where the amplitude is 20  
144 km/s. Additionally, if the interval time between two events is less than 20 minutes and they have similar  
145 frequency (within 0.5 mHz), we consider them as a single event.

146 The process of selecting wave events and distinguishing the wave mode in this study is as follows.  
147 Firstly, we conduct wavelet analysis to THEMIS ion velocity and magnetic field data in GSM coordinates  
148 and choose the wave events which roughly to satisfy the criteria mentioned above. Then, we transform  
149 from GSM to FAC coordinates for magnetic field and ion velocity data, and calculate the electric field.  
150 To quantitatively distinguish the azimuthal or radial oscillating waves, Fast Fourier Translation (FFT)  
151 analysis is applied to all three components of ion velocity (Fig. 2).

152 Figure 2 shows two typical events (labelled “A” and “B”) with Event A occurring near  $R\approx 19 R_E$ ,  
153 from 0550 to 0650 UT on 01 February 2009 and showing azimuthal oscillations, and Event B occurring  
154 near  $R\approx 8 R_E$  from 0728 to 0828 on 11 April 2013 and showing radial oscillations. Figure 2 shows three  
155 components of the ion velocity (a-c), magnetic field (d-f), and the calculated electric field (g-i), in addition  
156 to the total ion density (j) and total magnetic field (k) which are used for excluding mirror-like structures.  
157 Figure 2(l-n) show the Power Spectral Density (PSD) of the three components of the ion velocity derived  
158 by FFT. **Only events with an obvious single spectral peak, similar to events A and B, are considered as a**  
159 **“quasi monochromatic” wave and selected in our list of events.** In events A and B, the peak in PSD of the  
160 dominant wave component exceeds its counterpart by a factor of 4, enabling their unambiguous  
161 designation as an azimuthal and radial oscillation event respectively. Events for which the peak in PSD  
162 in  $V_a$  and  $V_r$  have similar magnitudes are simply regarded as both an azimuthal oscillating event and a  
163 radial oscillating event. **Note that the magnetic field vector used for calculating  $\mathbf{E}$  ( $\mathbf{E} = -\delta\mathbf{V}\times\mathbf{B}$ ) at each**  
164 **moment may deviate from the z-axis determined by 30 minutes sliding average of the magnetic field**  
165 **data. Therefore, the  $E_z$  component will have a small deviation from zero in the FAC coordinate system**  
166 **as shown in Fig. 2g.**



167

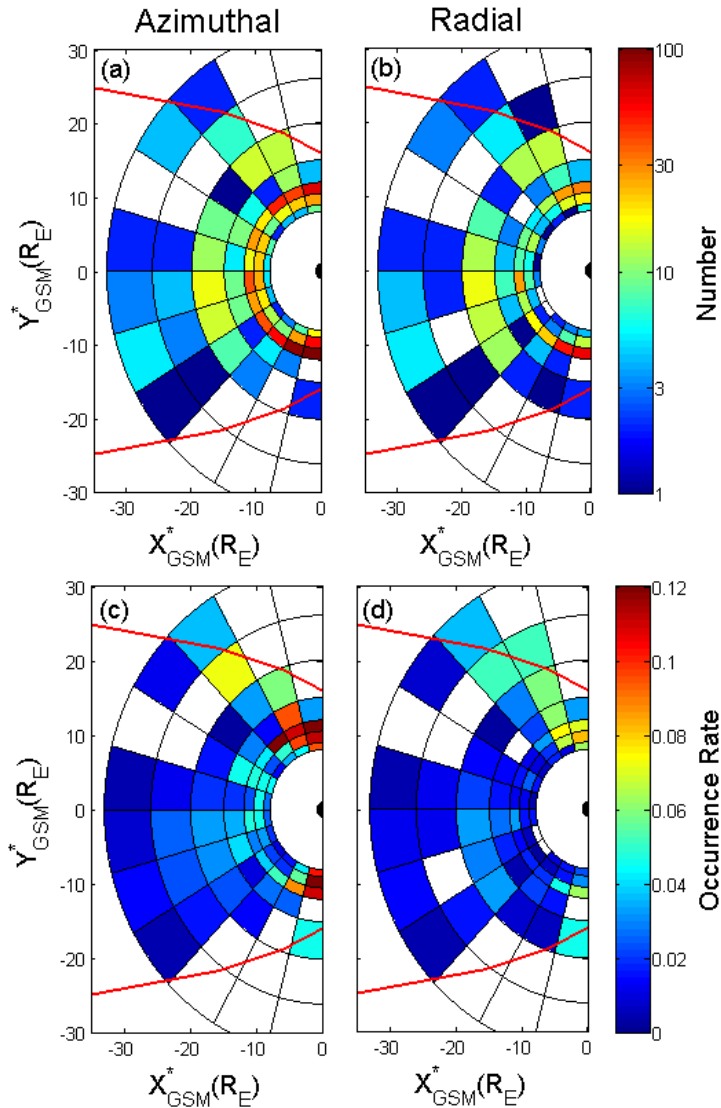
168 **Figure2.** Examples of an azimuthal oscillating event (Event A) from 0550 to 0650 UT on 01 February  
 169 2009, and radial oscillating event (Event B) from 0728 to 0828 on 11 April 2013: (a-c) velocity  
 170 components, (d-f) magnetic components, (g-i) electric field components, (j) total ion density, (k)  
 171 total magnetic field, (l-n) FFT analysis of ion velocity.

172 In total, we find 1089 azimuthal oscillating wave events and 566 radial oscillating wave events, with  
173 an average event-time duration of  $\sim 54$  minutes. Figure 3a and 3b shows the spatial distribution of the  
174 number of events in the GSM\* X-Y plane, both for azimuthal (left panel) and radial (right panel)  
175 oscillating wave events. The blank bins inside the magnetopause indicates that there are no events.  
176

### 177 3 Statistical Analysis

#### 178 3.1 Occurrence rate

180  
181 Figure 3c and 3d shows the occurrence rates of azimuthal oscillating wave events (left panel) and radial  
182 oscillating wave events (right panel) in the GSM\* X-Y plane. The color indicates the occurrence rate  
183 calculated by dividing the total duration of all events by the total duration of observations in each bin  
184 shown in Fig. 1. The blank bins inside the magnetopause indicates that there are no events. In the near-  
185 earth region ( $8 R_E < R < 12 R_E$ ), we can see that the occurrence rates of both azimuthal and radial  
186 oscillating events in the dusk and dawn flanks (18-21 MLT and 3-6 MLT) are higher than the midnight  
187 regions (21-03 MLT). For radial oscillating events, the occurrence rates of waves are higher on the  
188 duskside than dawnside. For azimuthal oscillating events, the dawn-dusk asymmetry in the occurrence  
189 rates is less clear than that for radial oscillating events. In the magnetotail region ( $12 R_E < R < 32 R_E$ ), the  
190 occurrence rates of both modes of waves are slightly higher in the post-midnight region. Note that,  
191 although no wave events are found in the dawnside flank region ( $20 R_E < R < 32 R_E$ , 3-6 MLT), the total  
192 observation time is also very short ( $< 38$  hours) in this region. So, we cannot conclusively say that the  
193 occurrence rates on the duskside flank region is higher than that of the dawnside.



194

195 **Figure 3.** The **number** (a and b) and **occurrence rates** (c and d) of azimuthal oscillating wave events (left  
 196 panel) and radial oscillating wave events (right panel) in the GSM\* X-Y plane.

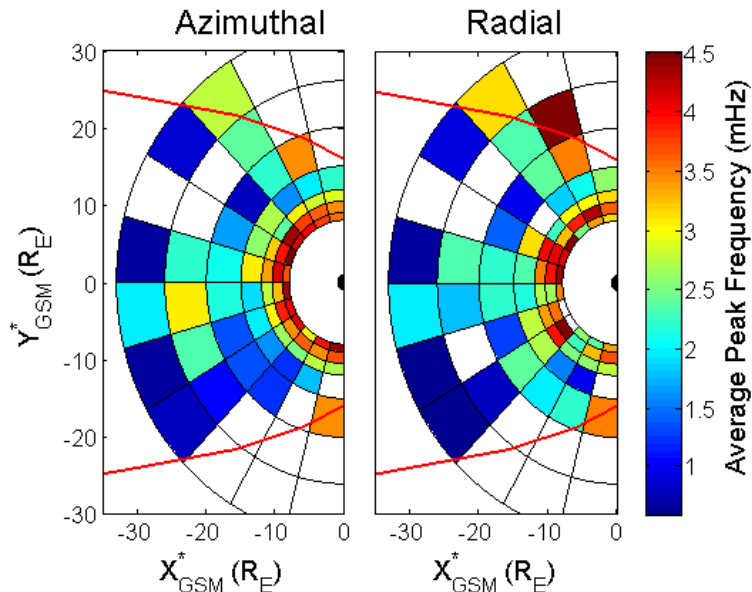
197

### 198 3.2 Frequency distribution

199

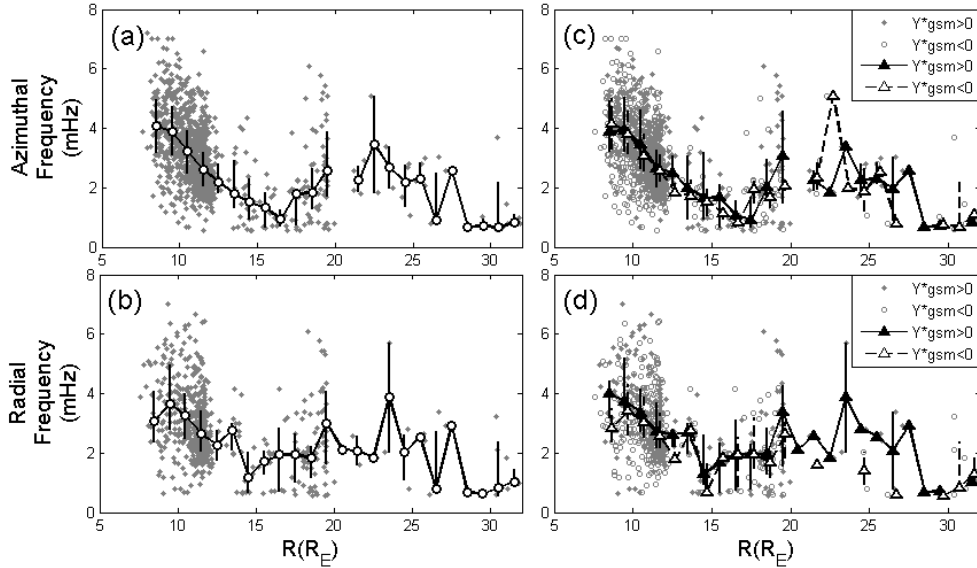
200 Figure 4 shows the spatial distribution of average frequency for azimuthal (left panel) and radial (right  
 201 panel) oscillating wave events in the equatorial plane. The color in each bin is the average of all event  
 202 frequencies (obtained by FFT analysis as described earlier) in that bin. A blank bin inside the  
 203 magnetopause indicates that there are no events. It can be seen roughly that the frequency decreases with

204 increasing radial distance both for azimuthal and radial oscillating wave events, for regions where  
 205  $R < 15R_E$ . Note that the crimson bin in the upper right corner (19-20 MLT and  $20 < R < 26 R_E$ ) of the right  
 206 panel is caused by short residence time ( $\sim 19$  hours) and only one wave event with frequency of 5.71 mHz.



207  
 208 **Figure 4.** The average frequencies of azimuthal oscillating wave events (left panel) and radial oscillating  
 209 wave events (right panel) in the GSM\* X-Y plane.

210  
 211 We further plot the relationship between the peak frequency and the distance from Earth in Fig. 5. It  
 212 shows that the frequency can be as low as 0.55 mHz. As shown in Fig. 5a and 5b, the median frequency  
 213 of azimuthal oscillating events decreases with increasing radial distance from the Earth in the region with  
 214  $8 R_E < R < 16 R_E$ , and the same trend is found for the radial oscillating events with  $8 R_E < R < 14 R_E$ .  
 215 Figure 5c and 5d show frequency distribution of events in the **dawnside** ( $Y^*_{gsm} < 0$ ) and **duskside** ( $Y^*_{gsm} >$   
 216  $0$ ) regions, respectively. The frequency for both azimuthal and radial oscillating events show no obvious  
 217 dawn dusk asymmetry. This is verified by the Wilcoxon rank sum test applied to the dawn and dusk  
 218 datasets. The Wilcoxon rank sum test is a non-parametric statistical hypothesis test that can be used to  
 219 assess whether two samples have the same distribution or not (Gibbons and Chakraborti, 2011).  
 220 Specifically, in the Wilcoxon rank sum test, a “P-value” result greater than 0.01 means there is no  
 221 significant statistical difference between two datasets. The P-value for the dawn and dusk side data sets  
 222 is 0.4535 (for all azimuthal and radial oscillating events). This confirms that the dawn and dusk side  
 223 frequency data sets belong to the same distribution.



224

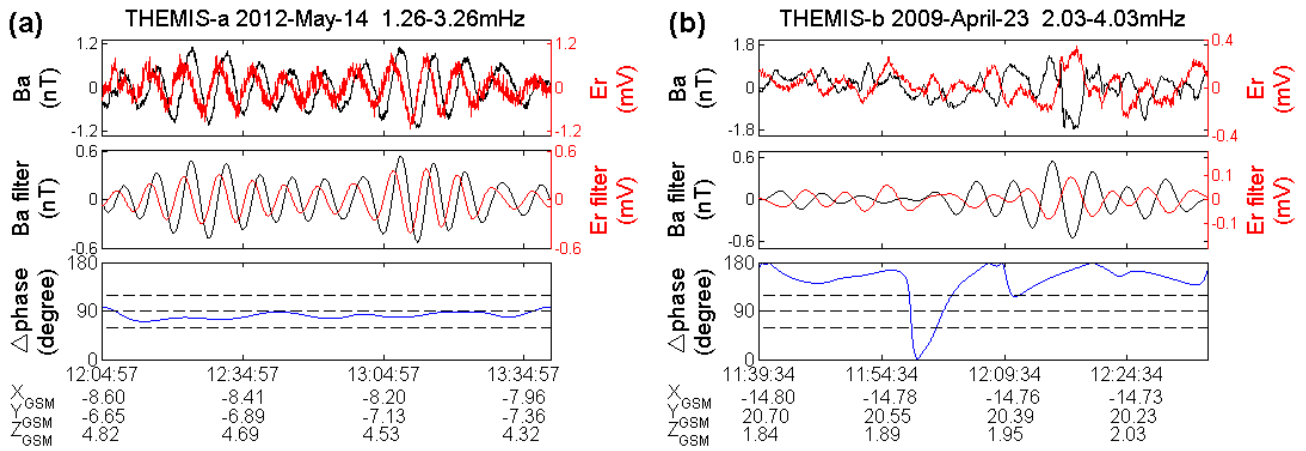
225 **Figure 5.** The wave frequency versus radial distance for azimuthal (a and c) and radial (b and d) oscillating  
 226 event. In panels a and b, the grey dots are individual events, the open circles are the median values of  
 227 frequencies in each 1  $R_E$  bin. The vertical bars connect the lower and upper quartiles. In panel c and d, the  
 228 grey dots and circles indicate the dusk and dawn events, respectively. The solid and open triangles are the  
 229 same as the open circles in Fig. 5a, but for dusk and dawn events respectively.

230

### 231 3.3 Standing wave

232

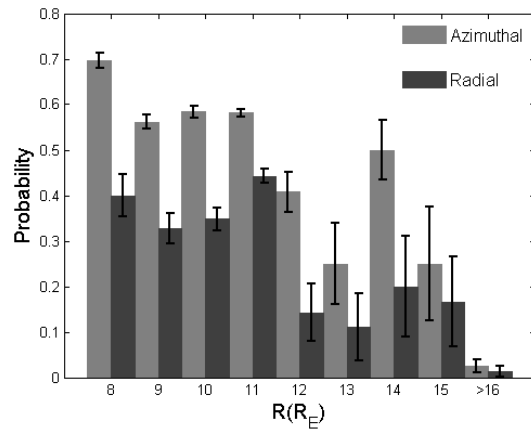
233 According to Singer et al. (1982), Alfvénic standing wave oscillations are characterized by a phase  
 234 difference of  $90^\circ$  between the electric field and magnetic field components. Figure 6 shows the standing  
 235 wave analysis of two azimuthal oscillating events. The first row shows the magnetic field component  $B_a$   
 236 and electric field component  $E_r$ . The second row shows the 1.26-3.26 mHz (Fig. 6a) and 2.03-4.03 mHz  
 237 (Fig. 6b) band-pass filtered  $B_a$  and  $E_r$  components. **The lower (upper) limits of the frequency bands are**  
 238 **obtained by subtracting (adding) 1 mHz from the peak frequencies in Fig. 2(l-n).** The **absolute value of**  
 239 **the phase differences** between the band-pass filtered  $B_a$  and  $E_r$  are shown in the bottom panels, in which  
 240 three dotted lines indicate the  $60^\circ$ ,  $90^\circ$ ,  $120^\circ$  phase differences respectively. We can see that the first event  
 241 (Fig. 6a) shows characteristics of standing wave as indicated by the  $\sim 90^\circ$  phase difference between  $E_r$   
 242 and  $B_a$ , while the second event (Fig. 6b) does not have this characteristic. We quantify the criteria of  
 243 standing azimuthal (radial) oscillating waves as that the **absolute value of the phase differences** between  
 244 the filtered  $B_a$  and  $E_r$  ( $B_r$  and  $E_a$ ) that falls within the range  $60^\circ$ - $120^\circ$  and lasts for at least three cycles.



245 **Figure 6.** Examples of: (a) a standing azimuthal oscillating event and (b) a non-standing azimuthal  
 246 oscillating event.  
 247

248  
 249 **Figure 7** shows the radial distribution of the probability that a given azimuthal or radial oscillating  
 250 wave event shows signatures of a standing wave. The light and dark histogram represents the probability  
 251 for azimuthal and radial oscillating event respectively. The errorbars shown are calculated by  $\epsilon = \frac{n}{N} *$

252  $\left(\frac{\sqrt{n}}{n} + \frac{\sqrt{N}}{N}\right)$ , where n is the number of standing wave events and N is the total number of waves events in  
 253 each bin for each polarization. It is obvious that standing waves occupy a larger proportion in the region  
 254 of 8-16 R<sub>E</sub>, while almost no standing waves are identifiable in the region of 16-32 R<sub>E</sub>. We find that about  
 255 52% events (including the azimuthal and radial oscillating events) are standing waves in the region of 8-  
 256 16 R<sub>E</sub>, while only 2 % are standing waves in the region of 16-32 R<sub>E</sub>. This figure also shows that the  
 257 probability of standing waves is higher for the azimuthal oscillating events than for the radial oscillating  
 258 events.



259  
 11



260 **Figure 7.** The radial distribution of the probability of identifying standing waves, for azimuthal and radial  
261 oscillating events (light and dark histograms respectively).

262

## 263 **4 Discussion**

264

265 Using THEMIS data during the period from 2008 to 2015, we find 1314 Pc5-6 ULF wave events in the  
266 region of  $X_{\text{GSM}}^* < 0$  and  $8 R_E < R < 32 R_E$ . The elevation angle of the magnetic field of each event was

267 calculated by the formula  $\tan^{-1}\left(\frac{B_z}{\sqrt{B_x^2+B_y^2}}\right) * \frac{180}{\pi}$ , where  $B_x$ ,  $B_y$ ,  $B_z$  are the three magnetic field

268 components in GSM\* coordinates. We find that 61.70% of the events have an elevation angle larger than

269  $45^\circ$  and only 2.48% events with an elevation angle less than  $10^\circ$ . This suggests that most of our events

270 are observed near the magnetic equatorial plane. The harmonic mode of each event was identified by the

271 E-B phase difference and the magnetic latitude. We find that only 2.90% wave events may be second

272 harmonic waves. It is reasonable to consider that most of our standing wave events belong to the

273 fundamental eigenmode. In this study, the ion velocity data used to identify ULF waves are usually

274 reliably measured in the plasma sheet. Furthermore, Lui and Cheng. (2001) indicated that the magnetic

275 field lines in the nightside are very stretched in the region of  $R > 8 R_E$ , especially during intervals of high

276 Kp index. We therefore consider it likely that most of our events should be observed on stretched magnetic

277 field lines, but not on open magnetic field lines.

278

### 279 **4.1 Occurrence rate**

280

281 As shown in Fig. 3c and 3d, in the region of  $8 R_E < R < 12 R_E$ , the occurrence rates are higher on the

282 duskside than dawnside for radial oscillating waves, while the dawn-dusk asymmetry in the occurrence

283 rates is less clear for azimuthal oscillating waves than that for radial oscillating waves. This is consistent

284 with the wave mode distributions in the inner magnetosphere ( $4 R_E < R < 9 R_E$ ) presented in previous

285 works (Hudson et al., 2004, Liu et al., 2009). One possible reason is that westward drifting ions injection

286 associated with substorm may excite more radial oscillating wave events in the duskside via the ion drift

287 bounce resonance (Southwood et al., 1969; Chen and Hasegawa, 1988). However, Takahashi et al. (2014)

288 found that the occurrence rate of toroidal waves is higher on the dawnside than duskside, which is different

289 from our result. We noticed that they only focused on the pure toroidal wave, while azimuthal oscillating

290 waves with comparable power in  $V_a$  and  $V_r$  are also included in our list of events. Thus, more azimuthal

291 oscillating waves could be observed in the duskside because of the possible coupling between azimuthal

292 oscillating waves and radial oscillating waves (with higher occurrence in the dusk sector). In contrast to

293 that of the inner magnetosphere ( $4 R_E < R < 9 R_E$ ), the occurrence rates for both azimuthal and radial

294 oscillating events in the region of  $12 R_E < R < 32 R_E$  are slightly higher on the post-midnight region than

295 the pre-midnight region. It is possible that the K-H instability may play an important role on the generation

of ULF waves on the stretched magnetotail, given that the K-H instabilities are **more** inclined to occur in the **dawnside** than in the **duskside** (Nykyri et al., 2013) and even can happen in the down tail flanks up to the lunar orbit ( $\sim 60 R_E$ ) (Wang et al., 2017). In view of the limited observation times in the **dawnside** magnetopause, more events are needed **to** further study on the definite reasons of the dawn-dusk asymmetry of occurrence rate in the outer side region ( $12 R_E < R < 32 R_E$ ).

## 4.2 Frequency distribution

As shown in Fig. 5a and 5b, the frequency decreases with increasing radial distance from the Earth for both azimuthal oscillating events ( $8 R_E < R < 16 R_E$ ) and radial oscillating events ( $8 R_E < R < 14 R_E$ ). This is consistent with the **Alfvén** continuum of field line resonance (FLR) theory (e.g., Allan and **Poulter**, 1992; Waters et al., 2000). However, this trend does not continue for  $R > 16 R_E$ . Previous observation and simulation studies have shown that standing waves can exist on the stretched magnetic field lines (Lui and Cheng, 2001; Zheng et al., 2006; Tian et al., 2012). Our statistical result shows that 52 % of all event types are standing waves in the region of 8-16  $R_E$ , while only 2 % can be confirmed as standing waves in the region of 16-32  $R_E$  as shown in Fig. 7. Given the likelihood that most of our wave events belong to the fundamental mode, the uncertainty in the phase measurement of the weak magnetic field signal near the equatorial plane will affect the identification of standing waves. Moreover, the complicated phase relationship between the electric field and the magnetic field caused by magnetic field disturbances in the farther deeper magnetotail will also affect the identification of standing waves. These suggest that our data may underestimate the proportion of standing wave events. Even so, the finding that only 2 % of events in the down-tail region ( $R > 16 R_E$ ) can be identified as standing waves suggests that the standing waves are far less common on the highly stretched field lines.

As shown in Fig. 5c and 5d, there is no obvious dawn-dusk asymmetry in the ULF wave frequency for  $8 R_E < R < 32 R_E$ . This is different from previous studies in the near-earth region (Liu et al., 2009; Takahashi et al., 1982; 2015). Takahashi et al. (1982) found that the frequencies of Pc3-4 ULF waves were higher on the **dawnside** than **duskside** at geosynchronous orbit. They suggested that the quasi-parallel shock and the associated turbulent magnetosheath flow is more likely to occur on the **dawnside**, which leads to higher harmonic waves to be excited in the **dawnside**. Takahashi et al. (2015) found that the frequencies of Pc5 toroidal waves in the region with L values between 7 and 12  $R_E$  is lower in the **duskside** (16-20 MLT) than **dawnside** (04-08 MLT). They suggest that this is due to the higher mass density in the **duskside** near-earth region, supplied by the particles from ionosphere. However, the wave frequency distributions shown in this paper ( $X_{GSM}^* < 0$ ,  $8 R_E < R < 32 R_E$ ) show a different distribution feature from that of the events in the inner or dayside magnetosphere. This suggests that neither of the above mechanisms for producing asymmetry are important within the region of interest in our study. This may be expected for the turbulent magnetosheath flow mechanism more applicable to higher frequencies. The influence of particle injection from the ionosphere may be weakened by higher ExB drift speeds and

333 longer field line lengths in the nightside magnetotail region, compared to the near-earth region.

### 334 4.3 The influence of Solar wind parameters and geomagnetic activity level

336 Figure 8a and 8b shows the relationship between the occurrence rate of wave events and solar wind velocity  $V_x$  and AE index. The Y-axis indicates the probability of detecting one wave event in each bin. The background solar wind data is obtained from OMNI from 2008 to 2015. We can see that the ULF wave occurrence increases with increasing solar wind speed  $|V_x|$ . This implies that the K-H instability could be a source of ULF waves in the magnetotail region (8-32  $R_E$ ), since the higher shear velocity is an important factor for exciting K-H instabilities (Miura, 1992). Figure 8b shows that the wave occurrence is higher when the AE values are less than 500 nT. Note that about 74.8 % of the waves occurred when the AE values are less than 250 nT. This suggests that most of the wave events in the magnetotail are observed during quiet times or weak substorm times. Figure 8c and 8d shows the relationship between the occurrence of ULF waves and the relative variation of solar wind dynamic pressure ( $P_d$ ) and the IMF  $B_z$  values. The relative variation of  $P_d$  for a given event is calculated by the formula  $\frac{P_{d_{max}} - P_{d_{min}}}{P_{d_{mean}}}$ , where  $P_{d_{max}}$ ,  $P_{d_{min}}$ ,  $P_{d_{mean}}$  denote the maximum, minimum and mean value of the solar wind  $P_d$  within a 30 minute window, starting 20 min before the beginning time of this event. We find that the occurrence rates are higher for larger solar wind  $P_d$  variance and during periods of northward IMF  $B_z$ .

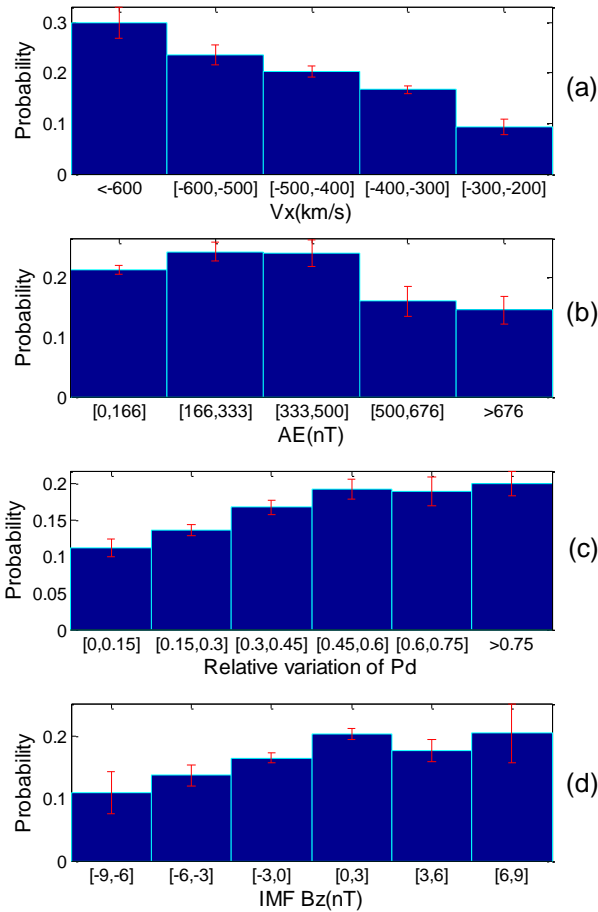
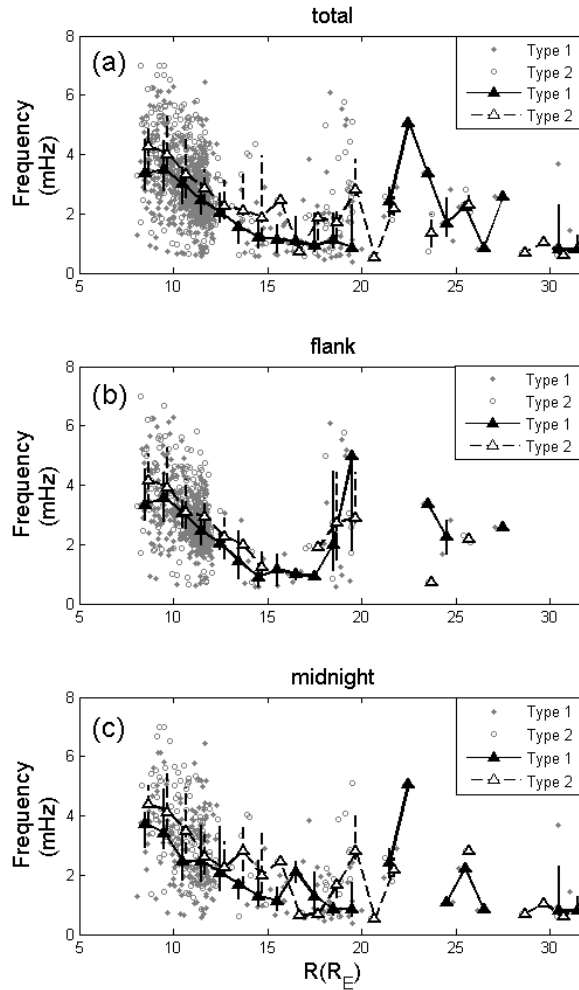


**Figure 8.** The occurrence probability of waves versus (a) Solar wind velocity  $V_x$ , (b) AE index, (c) Relative variation of  $P_d$ , and (d) IMF  $B_z$ .

The possibility that substorm activity may affect the frequency of ULF waves, and thereby influence the distribution of ULF frequencies in our database, is examined using the following method, based on the substorm event list of Forsyth et al. (2015). The ULF wave events were divided into two categories based on their start time relative to the onset time of individual substorm events. The first category (“type one”) consists of events that occurred more than two hours after the most recent substorm onset, and more than one hour before the next substorm onset. These events are considered to be independent of substorm activity. The second category (“type two”) consists of events that occurred between zero and two hours after the most recent substorm onset. In principle a third category consisting of events that occur less than

363 one hour before the next substorm onset could be defined, however this category contains very few events,  
364 so their frequency characteristics will not be discussed here. The radial dependence of median frequency  
365 for type one and two events is shown in Fig. 9a. This plot clearly shows that the median frequencies for  
366 type two events are higher than type one events. A plausible explanation for this difference could be that  
367 field line depolarization following substorm onset results in an increase in local magnetic field strength  
368 compared to more stretched magnetotail field lines during quiet times. The resulting higher Alfvén speed  
369 profile raises the fundamental mode eigenfrequency for the type two events, compared to the type one  
370 events.

371 Figure 9b and 9c show the radial dependence of median frequency for type one and two events  
372 occurring in the dawn/dusk flank (3-6 MLT and 18-21 MLT) and midnight sectors (21-03 MLT),  
373 respectively. According to these plots, the frequency differences between type one and type two wave  
374 events are more obvious in the midnight region than in the flank region. This is understandable, given  
375 that the configuration of field lines will be changed much more in the midnight region than in the flank  
376 regions during substorm times. It should be noted that, only the possible influence of field lines  
377 configuration or plasma environment associated with weak substorms on the ULF wave frequencies are  
378 discussed here. The question of whether substorms could trigger or be triggered by ULF waves still cannot  
379 be answered by the present analysis.



380

381 **Figure 9.** The wave frequency versus the distance from the earth for: (a) the type one and type two wave  
 382 events, (b) the wave events in the flank region, and (c) the wave events in the midnight region, respectively.  
 383 The grey dots and circles indicate type one and type two wave individual events respectively. The solid  
 384 and open triangles are the median values of frequencies in each  $1R_E$  bin for the type one and type two  
 385 wave event respectively. The vertical bars connect the lower and upper quartiles for each category.

386

### 387 5 Summary

388

389 We have statistically studied the distributions of the occurrence rate and frequency of the Pc5-6 ULF  
 390 waves in the region of  $X_{GSM}^* < 0$  and  $8 R_E < R < 32 R_E$  (occurring mostly on stretched magnetic field

391 lines) using 8 years of THEMIS data. We also examined the influence of Solar wind parameters and  
392 geomagnetic activity level on the features of these ULF waves. Some new results that differ from those  
393 of ULF waves observed in the inner magnetosphere are obtained. The main results are summarized as  
394 follows:

395 (1) In the far magnetotail region ( $12 R_E < R < 32 R_E$ ), the occurrence rates of both azimuthal and  
396 radial oscillating events are higher in the post-midnight region than in the pre-midnight region. In the  
397 near-earth magnetotail ( $8 R_E < R < 12 R_E$ ), **the occurrence rates of radial oscillating events are higher on**  
398 **the duskside, while the dawn-dusk asymmetry in the occurrence rates of azimuthal oscillating events are**  
399 **less clear than that of radial oscillating events**, which is similar to the distributions in the inner  
400 magnetosphere ( $4 R_E < R < 9 R_E$ ).

401 (2) Statistically, the peak frequency decreases **with increasing** radial distance from Earth for both  
402 azimuthal oscillating events ( $8 R_E < R < 16 R_E$ ) and radial oscillating events ( $8 R_E < R < 14 R_E$ ). A possible  
403 explanation for this distribution is that at least 52 % events (including both azimuthal and poloidal  
404 oscillating events) are standing waves in the region of 8-16  $R_E$ , while only 2 % are unambiguous standing  
405 waves in the region of 16-32  $R_E$ . Moreover, the frequencies for all the events in this paper do not show  
406 obvious dawn-dusk asymmetry **contrary to results from** previous studies for waves in the inner  
407 magnetosphere ( $4 R_E < R < 9 R_E$ ), where the wave frequencies are higher in the **dawnside** than in the  
408 **duskside**.

409 (3) The ULF wave occurrence rates are higher for larger solar wind velocity and solar wind Pd  
410 variations. Therefore, we suggest that the solar wind **may be** the main energy source of the ULF waves in  
411 the region of  $8 R_E < R < 32 R_E$ . About 74.8 % of the ULF waves occurred when the AE values are less  
412 than 250nT, which indicates that the ULF waves **are** most likely to occur during in the quiet times or weak  
413 substorm times. We have further studied the frequency change between the quiet time and the weak  
414 substorm time events. We found that the wave frequency is higher during the substorm time (0-2 hours  
415 after substorm onset). The frequency differences are clearer in the midnight region than in the flank region.  
416 We suggest that the field lines configuration or plasma environment variation during weak substorm times  
417 could increase the eigen frequencies of ULF waves in the magnetotail, leading to the observed change in  
418 the frequency distribution.

419  
420 *Acknowledgments.* We acknowledge THEMIS project team for THEMIS data at  
421 <http://themis.ssl.berkeley.edu/>, and SPDF web service for OMNI data at <https://spdf.sci.gsfc.nasa.gov/>.  
422 This work was supported by the Shandong University (Weihai) future plan for Young Scholar  
423 (2017WHWLJH08), the National Natural Science Foundation of China (Grants Nos. 41304129,  
424 41774153, 41574157, and 41628402), the Science and Technology Facilities Council (Grants Nos.  
425 ST/N000722/1), Natural Environment Research Council (Grants Nos. NE/L007495/1, NE/P017150/1 and  
426 NE/P017185/1). Project Supported by the Specialized Research Fund for State Key Laboratories.

427

428 **Reference**

- 429 Allan, W., White, S. P., and Poulter, E. M.: Impulse-excited hydromagnetic cavity and field-line  
430 resonances in the magnetosphere, *Planet. Space Sci.*, 34, 371–385, doi:10.1016/0032-  
431 0633(86)90144-3, 1986.
- 432 Allan, W. and Poulter, E. M.: Ulf waves-their relationship to the structure of the earth's magnetosphere,  
433 *Rep. Prog. Phys.*, 55(55), 533-598, doi:10.1088/0034-4885/55/5/001, 1992.
- 434 Angelopoulos, V.: The THEMIS mission, *Space Sci. Rev.*, 141, 5–34, doi:10.1007/s11214-008-9336-1,  
435 2008.
- 436 Auster, H. U., Glassmeier, K. H., Magnes, W., Aydogar, O., Baumjohann, W., Constantinescu, D.,  
437 Fornacon, K. H., Georgescu, E.; Harvey, P., Hillenmaier, O., Kroth, R., Ludlam, M., Narita, Y.,  
438 Nakamura, R., Okrafka, K., Plaschke, F., Richter, I., Schwarzl, H., Stoll, B., Valavanoglou, A., and  
439 Wiedemann, M.: The Themis fluxgate magnetometer, *Space Sci. Rev.*, 141(1-4), 235-264,  
440 doi:10.1007/s11214-008-9365-9, 2008.
- 441 Baumjohann, W. and Glassmeier, K. H.: The transient response mechanism and Pi2 pulsations at substorm  
442 onset: Review and outlook, *Planet. Space Sci.*, 32, 1361–1370, doi:10.1016/0032-0633(84)90079-5,  
443 1984.
- 444 Chen, L. and Hasegawa, A.: On magnetospheric hydromagnetic waves excited by energetic ring current  
445 particles, *J. Geophys. Res.*, 93, 8763, 1988.
- 446 Claudepierre S. G., Elkington, S. R., and Wiltberger, M.: Solar wind driving of magnetospheric ULF  
447 waves: Pulsations driven by velocity shear at the magnetopause, *J. Geophys. Res.*, 113: A05218,  
448 2008.
- 449 Degeling, A. W., Rankin, R., and Zong, Q.-G.: Modeling radiation belt electron acceleration by ULF fast  
450 mode waves, launched by solar wind dynamic pressure fluctuations, *J. Geophys. Res. Space Physics*,  
451 119, 8916–8928, doi:10.1002/2013JA019672, 2014.
- 452 Forsyth, C., Rae, I. J., Coxon, J. C., Freeman, M. P., Jackman, C. M., Gjerloev, J., and Fazakerley, A. N.:  
453 A new technique for determining Substorm Onsets and Phases from Indices of the Electrojet  
454 (SOPHIE), *J. Geophys. Res. Space Physics*, 120, 10,592–10,606, doi:10.1002/2015JA021343, 2015.
- 455 Gibbons, J. D., and Chakraborti, S.: *Nonparametric Statistical Inference*, 5th Ed., Boca Raton, FL:  
456 Chapman & Hall/CRC Press, Taylor & Francis Group, 2011.
- 457 Hudson, M. K., Denton, R. E., Lessard, M. R., Miftakhova, E. G., and Anderson, R. R.: A study of Pc-5  
458 ULF oscillations, *Ann. Geophys.*, 22, 289, 2004.
- 459 Kepko, L., Spence, H. E., and Singer, H. E.: ULF waves in the solar wind as direct drivers of  
460 magnetospheric pulsations, *J. Geophys. Res.*, 29, 39-1, 2002.
- 461 Kepko, L. and Spence, H. E.: Observations of discrete, global magnetospheric oscillations directly drive  
462 n by solar wind density variations, *J. Geophys. Res.*, 108(A6), 1257, doi:10.1029/2002JA009676, 2  
463 003.
- 464 Keiling, A.: Alfvén Waves and Their Roles in the Dynamics of the Earth’s Magnetotail: A Review, *Space*



465 Sci. Rev., 142:73-156, 2009.

466 Lee, D., and Lysak, R. L.: Magnetospheric ulf wave coupling in the dipole model: the impulsive excitation,  
 467 J. Geophys. Res. Space Physics, 94(A12), 17097-17103, 1989.

468 Lessard, M. R., Hudson, M. K., and Luhr, H.: A statistical study of Pc3 –Pc5 magnetic pulsations observed  
 469 by the AMPTE/Ion Release Module satellite, J. Geophys. Res., 104, 4523, doi:10.1029/  
 470 1998JA900116, 1999.

471 Liu, W., Sarris, T. E., Li, X., Elkington, S. R., Ergun, R., Angelopoulos, V., Bonnell, J., and Glassmeier,  
 472 K. H.: Electric and magnetic field observations of Pc4 and Pc5 pulsations in the inner magnetosphere:  
 473 A statistical study, J. Geophys. Res., 114, A12206, doi:10.1029/2009JA014243, 2009.

474 Lui, A. T. Y. and Cheng, C. Z.: Resonance frequency of stretched magnetic field lines based on a self-  
 475 consistent equilibrium magnetosphere model, J. Geophys. Res., 106(A11), 25793–25802,  
 476 doi:10.1029/2001JA000113, 2001.

477 Miura, A.: Kelvin-Helmholtz Instability at the Magnetospheric Boundary: Dependence on the  
 478 Magnetosheath Sonic Mach Number, J. Geophys. Res., 97, 10 655, 1992.

479 Mcfadden, J. P., Carlson, C. W., Larson, D., Bonnell, J., Mozer, F., Angelopoulos, V., Glassmeier, K. H.,  
 480 and Auster, U.: THEMIS ESA first science results and performance issues, Space Sci. Rev., 141,  
 481 477–508, doi:10.1007/s11214-008-9433-1, 2008.

482 Nykyri, K.: Impact of MHD shock physics on magnetosheath asymmetry and Kelvin-Helmholtz  
 483 instability, J. Geophys. Res. Space Physics, 118, 5068–5081, doi:10.1002/jgra.50499, 2013.

484 Olson, J. V.: Pi2 pulsations and substorm onsets: A review, J. Geophys. Res., 104, 17,499–17,520,  
 485 doi:10.1029/1999JA900086, 1999.

486 Rae, I. J., Murphy, K. R., Watt, C. E. J., Rostoker, G., Rankin, R., Mann, I. R., Hodgson, C. R., Frey, H.  
 487 U., Degeling, A. W., and Forsyth, C.: Field line resonances as a trigger and a tracer for substorm  
 488 onset, J. Geophys. Res. Space Physics, 119, 5343–5363, doi:10.1002/2013JA018889, 2014.

489 Rankin, R., Fenrich, F. and Tikhonchuk, V. T.: Shear Alfvén waves on stretched magnetic field lines near  
 490 midnight in Earth’s magnetosphere, Geophys. Res. Lett., 27(20), 3265–3268, 2000.

491 Rostoker, G., Spadinger, I., and Samson, J. C.: Local time variation in the response of Pc 5 pulsations in  
 492 the morning sector to substorm expansive phase onsets near midnight, J. Geophys. Res., 89(A8),  
 493 6749–6757, doi:10.1029/JA089iA08p06749, 1984.

494 Samson, J. C. and Rostoker, G.: Response of dayside Pc 5 pulsations to substorm activity in the nighttime  
 495 magnetosphere, J. Geophys. Res., 86(A2), 733–752, doi:10.1029/JA086iA02p00733, 1981.

496 Saito, T.: Long-period irregular magnetic pulsation, Pi3, Space Sci. Rev., 21(4), 427–467,  
 497 doi:10.1007/BF00173068, 1978.

498 Shen, X. C., Zong, Q. -G., Shi, Q. Q., Tian, A. M., Sun, W. J., Wang, Y. F., Zhou, X. Z., Fu, S. Y., Hartinger,  
 499 M. D., and Angelopoulos, V.: Magnetospheric ULF waves with increasing amplitude related to solar  
 500 wind dynamic pressure changes: The Time History of Events and Macroscale Interactions during  
 501 Substorms (THEMIS) observations, J. Geophys. Res., 120(9): 7179-7190, doi:

10.1002/2014JA020913, 2015.

- 502  
503 Shen, X.C., Shi, Q. Q., Zong, Q.-G., Tian, A. M., Nowada, M., Sun, W. J., Zhao, H. Y., Hudson, M. K.,  
504 Wang, H. Z., Fu, S. Y., Pu, Z. Y.: Dayside magnetospheric ULF wave frequency modulated by a solar  
505 wind dynamic pressure negative impulse, *J. Geophys. Res. Space Physics*,  
506 122, doi:10.1002/2016JA023351, 2017.
- 507 Shi, Q. Q., Hartinger, M. D., Angelopoulos, V., Zong, Q.-G., Zhou, X.-Z., Zhou, X.-Y., Kellerman, A.,  
508 Tian, A. M., Weygand, J., Fu, S. Y., Pu, Z. Y., Raeder, J., Ge, Y. S., Wang, Y. F., Zhang, H., and Yao,  
509 Z. H.: THEMIS observations of ULF wave excitation in the nightside plasma sheet during sudden  
510 impulse events, *J. Geophys. Res.*, 118(1): 284-298, doi: 10.1029/2012JA017984, 2013.0
- 511 Shi, Q. Q., Hartinger, M. D., Angelopoulos, V., Fu, S. Y., Zong, Q. -G., Tian, A. M., Weygand, J. M.,  
512 Raeder, J., Pu, Z. Y., Zhou, X. Z., Dunlop, M. W., Liu, W. L., Zhang, H., Yao, Z. H., and Shen, X.  
513 C.: Solar wind pressure pulse-driven magnetospheric vortices and their global consequences, *J.*  
514 *Geophys. Res.*, 119(6): 4274-4280, doi: 10.1002/2013JA019551, 2014.
- 515 Shue, J.-H., Song, P., Russell, C. T., Steinberg, J. T., Chao, J. K., Zastenker, G., Vaisberg, O. L., Kokubun,  
516 S., Singer, H. J., Detman, T. R., and Kawano, H.: Magnetopause location under extreme solar wind  
517 conditions, *J. Geophys. Res.*, 103, 17691–17700, doi:10.1029/98JA01103, 1998.
- 518 Singer, H. J., Hughes, W. J., and Russell, C. T.: Standing hydromagnetic waves observed by ISEE 1 and  
519 2: Radial extent and harmonic, *J. Geophys. Res.*, 87, 3519–3529, 1982.
- 520 Southwood, D. J., Dungey, J. W., and Eherington, R. L.: Bounce resonant interaction between pulsations  
521 and trapped particles, *Planet Space Sci.*, 17, 349-361, 1969.
- 522 Sun, W. J., Slavin, J. A., Fu, S., Raines, J. M., Sundberg, T., and Zong, Q. -G., Jia, X. Z., Shi, Q. Q., Shen,  
523 X. C., Poh, G. K., Pu, Z. Y., and Zurbuchen, T. H.: Messenger observations of alfvénic and  
524 compressional waves during mercury's substorms. *Geophysical Research Letters*, 42(15), 6189-6198,  
525 2015.
- 526 **Kokubun, S.:** ULF waves in the outer magnetosphere: Geotail observation 1 transverse waves, *Earth*  
527 *Planets Space*, 65, 411-433, doi:10.5047/eps.2012.12.013, 2013.
- 528 Takahashi, K. and McPherron, R. L.: Harmonic structure of Pc3– 4 pulsations, *J. Geophys. Res.*, 87, 1504,  
529 doi:10.1029/JA087iA03p01504, 1982.
- 530 Takahashi, K. and Ukhorskiy, A. Y.: Solar wind control of Pc5 pulsation power at geosynchronous orbit,  
531 *J. Geophys. Res.*, 112, A11205, doi:10.1029/2007JA012483, 2007.
- 532 **Takahashi, K., Denton, R. E., Hirahara, M., Min, K., Ohtani, S., and Sanchez, E.:** Solar cycle variation of  
533 **plasma mass density in the outer magnetosphere: Magnetoseismic analysis of toroidal standing**  
534 **Alfvén waves detected by Geotail**, *J. Geophys. Res. Space Physics*, 119, 8338–8356,  
535 doi:10.1002/2014JA020274, 2014.
- 536 Takahashi, K., Hartinger, M. D., Angelopoulos, V., and Glassmeier, K. H.: A statistical study of  
537 fundamental toroidal mode standing Alfvén waves using THEMIS ion bulk velocity data, *J. Geophys.*  
538 *Res. Space Physics*, 120, 6474–6495, doi:10.1002/2015JA021207, 2015.

- 539 Tian, A. M., Zong, Q. -G., Zhang, T. L., Nakamura, R., Du, A. M., Baumjohann, W., Glassmeier, K. H.,  
540 Volwerk, M., Hartinger, M., Wang, Y. F., Du, J., Yang, B., Zhang, X. Y., and Panov, E.: Dynamics of  
541 long-period ULF waves in the plasma sheet: Coordinated space and ground observations, *J. Geophys.*  
542 *Res.*, 117, A03211, doi:10.1029/2011JA016551, 2012.
- 543 Ukhorskiy, A. Y., Takahashi, K., Anderson, B. J., and Korth, H.: Impact of toroidal ULF waves on the  
544 outer radiation belt electrons, *J. Geophys. Res.*, 110, A10202, doi:10.1029/2005JA011017, 2005.
- 545 Wang, G. Q., Zhang, T. L., and Ge, Y. S.: Spatial distribution of magnetic fluctuation power with period  
546 40 to 600 s in the magnetosphere observed by THEMIS, *J. Geophys. Res. Space Physics*, 120, 9281–  
547 9293, doi:10.1002/2015JA021584, 2015.
- 548 Wang, C.-P., Merkin, V. G., and Angelopoulos, V.: Mesoscale perturbations in midtail lobe/mantle during  
549 steady northward IMF: ARTEMIS observation and MHD simulation, *J. Geophys. Res.*, 122, 6430–  
550 6441, doi:10.1002/2017JA024305, 2017.
- 551 Walker, A. D. M.: The Kelvin-Helmholtz instability in the low-latitude boundary layer, *Planet. Space*  
552 *Science*, 29(10), 1119-1133, doi:10.1016/0032-0633(81)90011-8, 1981.
- 553 Waters, C. L., Harrold, B. G., Menk, F. W., Samson, J. C., and Fraser, B. J.: Field line resonances and  
554 waveguide modes at low latitudes: 2. A model, *J. Geophys. Res.*, 105(A4), 7763–7774,  
555 doi:10.1029/1999JA900267, 2000.
- 556 Yang, B., Zong, Q. -G., Wang, Y. F., Fu, S. Y., Song, P., Fu, H. S., Korth, A., Tian, T., and Reme, H.:  
557 Cluster observations of simultaneous resonant interactions of ULF waves with energetic electrons  
558 and thermal ion species in the inner magnetosphere, *J. Geophys. Res.*, 115, A02214,  
559 doi: 10.1029/2009JA014542, 2010.
- 560 Zhang, X. Y., Zong, Q. -G., Wang, Y. F., Zhang, H., Xie, L., Fu, S. Y., Yuan, C. J., Yue, C., Yang, B., and  
561 Pu, Z. Y.: ULF waves excited by negative/positive solar wind dynamic pressure impulses at  
562 geosynchronous orbit, *J. Geophys. Res.*, 115, A10221, doi: 10.1029/2009JA015016, 2010.
- 563 Zheng, Y., Lui, A. T., Mann, I. R., Takahashi, K., Watermann, J., Chen, S., Rae, I. J., Mukai, T., Russell,  
564 C. T., Balogh, A., Pfaff, R. F., and Reme, H.: Coordinated observation of field line resonance in the  
565 mid-tail, *Ann. Geophys.*, 24, 707–723, 2006.
- 566 Zong, Q. -G.: Ultralow frequency modulation of energetic particles in the dayside magnetosphere,  
567 *Geophys. Res. Lett.*, 34: L12105, 2007.
- 568 Zong, Q. -G., Wang, Y. F., Zhang, H., Fu, S. Y., Zhang, H., Wang, C. R., Yuan, C. J., and Vogiatzis, I.:  
569 Fast acceleration of inner magnetospheric hydrogen and oxygen ions by shock induced ULF waves,  
570 *J. Geophys. Res.*, 177, A11206, doi: 10.1029/2012JA018024, 2012.
- 571 Zong, Q. -G., Zhou, X. Z., Wang, Y. F., Li, X., Song, P., Baker, D. N., Fritz, T. A., Daly, P. W., Dunlop,  
572 M., and Pedersen, A.: Energetic electron response to ULF waves induced by interplanetary shocks  
573 in the outer radiation belt, *J. Geophys. Res.*, 114, A10204, doi:10.1029/2009JA014393, 2009.
- 574 Zong, Q. -G., Rankin, R. and Zhou, X. Z.: The interaction of ultralow frequency Pc 3-5 waves with  
575 charged particles in earth's magnetosphere, *Reviews of Modern Plasma Physics*, 1, 10,

